Research on burst gravitational waves with the Hilbert-Huang transform

Masato Kaneyama

Department of Physics, Osaka City University, Osaka, 558-8585, Japan

Ken-ichi Oohara, Takashi Wakamatsu

Graduate School of Science and Technology, Niigata University, Niigata 950-2181, Japan

Hirotaka Takahashi

Department of Information and Management Systems Engineering, Nagaoka Uniersity of Technology, Nagaoka, Niigata 940-2188, Japan and Earthquake Research Institute, The University of Tokyo, Bunkyo-Ku, Tokyo 113-0032, Japan

Jordan B. Camp

Laboratory for Gravitational Physics NASA Goddard Space Flight Center, Greenbelt, Maryland 20771, USA

The reconstruction of waveform is one of the most important issue of the parameter estimation of source in the GW astronomy. In this paper, we investigate a method of the waveform reconstruction of burst gravitational waves from a single detector's data using Hilbert-Huang Transform. Moreover, we demonstrate the wave reconstruction to confirm the effectiveness of our proposed method using the simulated data. As the results, we found that the reconstructed waveforms were obtained with good accuracy from only one detector data.

Keywords: Gravitational wave data analysis; Hilbert-Huang Transform; waveform reconstruction.

1. Introduction

The Hilbert-Huang transform (HHT), which consists of an empirical mode decomposition (EMD) followed by the Hilbert spectral analysis (HSA), was developed recently by Huang *et al.*[1]. The HHT can decompose any complicated date set via EMD into some intrinsic mode functions (IMFs) that admit a well-behaved Hilbert transform. Compared with the Fourier decomposition and wavelet decomposition, the EMD approach is fitter for analyzing the non-stationary data since it decomposes the signal based on the time scale of the signal itself with adaptive nature. Moreover, HHT is not limited by time-frequency uncertainty.

A waveform of burst gravitational waves (GWs) is difficult to predict from theoretical study. On the other hand, the physical parameters (e.g. the mass of progenitor model, pre-collapse rotation and equation of state etc.) are strongly reflected in the waveform[3] (See Fig.1). Therefore, the waveform reconstruction of burst GWs from noisy data obtained by observation is one of the most important issues to estimate parameters of supernovae etc. In this paper, we focus on the waveform reconstruction from a single detector's data by use of HHT.

We assume that the observational data $s(t)$ is given by sampling a continuous signal at discrete time series, $t_j = j\Delta t$ for $j = 0, 1, \cdots, N-1$, where N is the number of data points and Δt is the sampling interval and the observational data $s(t_j)$ is expressed by : $s(t_j) = h(t_j) + n(t_j)$, where $h(t_j)$ is the GW signal and $n(t_j)$ is the noise.

2. Outline of HHT

The HHT consists of two components. The first one is the EMD, which decomposes the time series data $s(t_j)$ into some Intrinsic Mode Functions (IMFs); IMF $c_i(t_j)$ $(i = 1, 2, \cdots)$. The EMD involves (1) forming an envelope about the data maxima and minima with the use of a cubic spline, (2) taking the average of the two envelopes, and then (3) subtracting it from the time series to obtain the residual. When iteration of this procedure converges, the residual is treated as an IMF. Subtracting it from the original time series, the procedure is carried out repeatedly to obtain succeeding IMFs. The sum of all IMF components restores the time series data to the original one : $s(t_j) = \sum_{i=1}^{M} c_i(t_j) + r(t_j)$, where M is the number of IMFs and $r(t_j)$ is the final residual, respectively.

In the second part of HHT, the Hilbert transform is applied to each IMF in order to derive the instantaneous frequency (IF) and the instantaneous amplitude (IA).

Detailed description of HHT used in this paper are found in Takahashi *et al.*[2].

3. Method of waveform reconstruction

By means of the EMD, the noise will be dispersed to all IMFs with equal amplitudes. On the other hand, the burst GW signal is expected to be decomposed to a few specific IMFs. In this point of view, by using the burst GW signal $h_i(t_j)$ and noise $n_i(t_j)$, IMFs $c_i(t)$ are given by :

$$c_i(t) = h_i(t_j) + n_i(t_j), \tag{1}$$

where $h(t_j) = \sum_{i=1}^{M} h_i(t_j)$ and $n(t_j) = \sum_{i=1}^{M} n_i(t_j)$.

We assume that the noise in each IMF is stationary and of normal distribution with zero mean and standard deviation σ_i. If we use X_i and Y_{ij} are the random variable of the noise and IMF, respectively, we can express :

$$n(t_j) : X_i \sim N(0, \sigma_i^2), \tag{2}$$

$$c_i(t_j) : Y_{ij} \sim N(\mu_{ij}, \sigma_i^2) = \mu_{ij} + N(0, \sigma_i^2). \tag{3}$$

If IMF $c_i(t_j)$ satisfies $|c_i(t_j)| > 4\sigma_i$, we consider this IMF $c_i(t_j)$ includes the component of signal. Then, we sum up these IMFs to get the reconstructed waveform:

$$\sum_i c_i(t_j) = h_{\mathrm{reconst}}(t_j) : W_j \sim N(\mu_j', \sigma'^2) = \mu_j' + N(0, \sigma'^2), \tag{4}$$

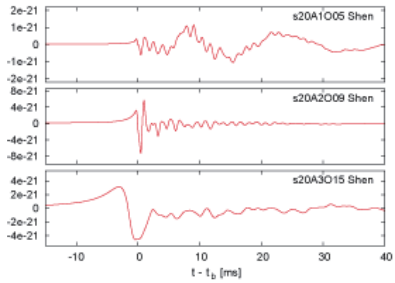

Fig. 1. Example of the waveforms at 10 kpc with changing initial rotation states, (other parameters are fixed). Note t_b is time of core bounce.

where W_j is its the random variable, $\mu'_j = \sum_i \mu_{ij}$ and $\sigma'^2 = \sum_{ik} \mathrm{Cov}(X_i, X_k)$ is covariance of summed up IMF. Therefore, we can obtain the reconstruct waveform μ'_j.

4. Setup for our data analysis simulation

To confirm the effectiveness of our proposed method, we demonstrate the wave reconstruction using the simulated data.

In this section, we explain the setup for our data analysis simulation. We prepare the simulated time-series data of Advanced LIGO by combining Gaussian noise with the burst gravitational waves from core collapse and core bounce of rotating stars obtained from Dimmelmeier's catalog[3].

With a sensitivity curve of Advanced LIGO (the zero-detuned, high-power sensitivity curve[4]), we produce the simulated Gaussian noise in frequency domain. The sampling frequency is set to $f_s = 1/\Delta t = 8192\,\mathrm{Hz}$ and the frequency range of the detector noise is set to be from 20 Hz to 4096 Hz. Time-series noise data, $n(t_j)$, is produced by the inverse Fourier transform of the simulated noise in frequency domain. We set the duration to be 0.5 s.

We use 136 gravitational waveforms from Dimmelmeier's catalog[3] and assign a serial number to each of them in the alphabetical order. For example, Fig. 1 shows the waveforms of different initial rotation states with other parameters fixed. We can find that the waveforms are very different and the physical parameters such as the mass of progenitor model, pre-collapse rotation, equation of state, and so on are strongly reflected in the waveform.

The observational data $s(t_j)$ is produced by injecting the GW signal $h_{\mathrm{catalog}}(t_j)$ into simulated time-series noise data of Advanced LIGO $n(t_j)$; $s(t_j) = h_{\mathrm{catalog}}(t_j) + n(t_j)$. In this paper, we consider gravitational waves entering from the optimal direction to the detector.

In the second column of the left of Fig.2(a), we show the example of $s(t_j)$. For each waveform, we created 1000 samples of $s(t_j)$, each of which is generated by adding a Gaussian random variate with a different seed.

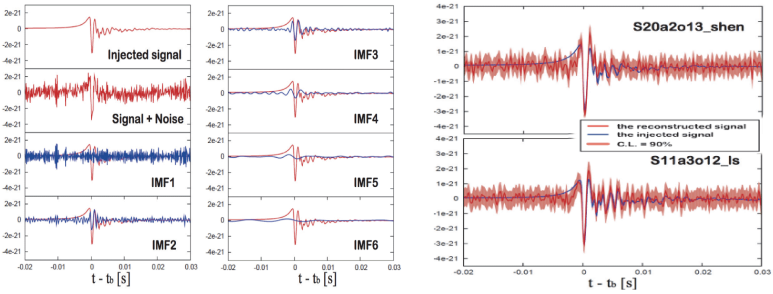

(a) (b)

Fig. 2. Example of results. (a) Injected signal (S20a2o13_shen) at 10 kpc, simulated Advanced LIGO noise plus signal and IMF1-IMF6. (b) Reconstructed and injected waveform.

5. Result

Figure 2(a) shows one of our results, where the signal of S20a2o13_shen in Dimmelmeier's catalog[3] at 10 kpc is injected in simulated time-series noise data of Advanced LIGO. The signal+noise data $s(t)$ was decomposed into 8 IMFs through Ensemble EMD[5]. We plot the IMF1-6 (blue) as well as injected signal (red) in Fig. 2(a). You can find that IMF2-4 contain the components of injected signal, while IMF1 has only noise.

Fig. 2(b) represents the injected signal (S20a2o13_shen and S11a3o12_ls) as blue lines, the reconstructed waveform as red lines and the 90% confidence level region as the red shaded regions. We found that the waveform reconstruction is possible with sufficient accuracy. For most of other injected signals in Dimmelmeier's catalog, we obtain the similar results.

To evaluate the degree of coincidence between injected signal $h_{\rm catalog}(t_j)$ and reconstructed waveform $h_{\rm reconst}(t_j)$, we calculate the value of reduced $\chi^2_{\rm red}$:

$$\chi^2_{\rm red} = \frac{1}{N'} \sum_{j=1}^{N'} \frac{[h_{\rm catalog}(t_j) - h_{\rm reconst}(t_j)]}{\sigma'^2}, \tag{5}$$

with the time duration of summation in Eq.(5) : $t - t_b = -20 \sim 50\ ms$ ($N' = 572$).

If each time point is independent, then this reduced $\chi^2_{\rm red}$ obey the χ^2 distribution with the mean 1 and variance $2/\sqrt{N'}$.

In order to calculate $\chi^2_{\rm red}$, we perform again the wave reconstruction for 1000 samples, each of which is generated by adding a Gaussian random variate. However, in this case, we use the injected signal at 25 kpc.

Fig. 3(a) shows the $\chi^2_{\rm red}$ as the function of the serial number of waveform, in the case that the reconstructed waveform is s20a2o09_shen at 25 kpc. The serial number 78 is the position of injected signal. The error bars show the 1 σ errors. The value of $\chi^2_{\rm red}$ of injected signal is smallest. This means the degree of coincidence between the reconstructed waveform and injected waveform is good. However, you can find that there are the positions (serial number 16, 44 and 78) of almost same

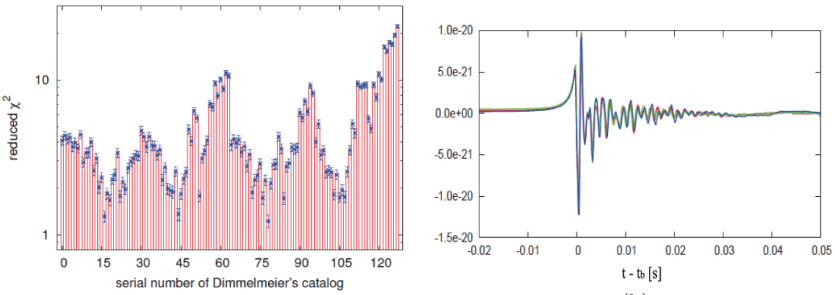

(a) (b)

Fig. 3. (a) $\chi^2_{\rm red}$ as the function of the serial number of waveform, in the case that the reconstructed waveform is s20a2o09_shen (serial number 78) at 25 kpc. The error bars show the 1 σ errors. (b) The injected waveforms of three serial numbers which have almost same value of $\chi^2_{\rm red}$.The red, green and blue curves show the waveform of s20a2o09_shen (serial number 78), s11a2o13_shen (serial number 16) and s15a2o07_shen (serial number 44) , respectively.

value of $\chi^2_{\rm red}$. We plot the injected waveforms of three corresponding serial numbers in Fig. 3(b) . We can find that the injected waveform is almost same waveform, which has different vale of parameters. This is reason why we have almost same value of $\chi^2_{\rm red}$.

For most of other injected signals in Dimmelmeier's catalog, we obtain the similar results. Thus, we conclude that the waveform reconstruction is possible with sufficient accuracy.

6. Summary

We presented a method of waveform reconstruction with the HHT. We used the 136 burst GW waveforms from Dimmelmeier's catalog[3] and the simulated time-series noise data of Advanced LIGO[4]. From the results of the wave reconstruction with HHT, the reconstructed waveforms with good accuracy were obtained from only one detector data. The physical parameters of rotating stars are likely to be determined with sufficient accuracy.

In this paper, we used simulated Gaussian noise of Advanced LIGO. However, the noise of real laser interferometer detectors show non-Gaussianity and non-stationarity. Therefore, we are planning to apply our method to real laser interferometer data in the near future.

Acknowledgments

This work was in part supported by MEXT Grant-in-Aid for Scientific Research on Innovative Areas "New Developments in Astrophysics Through Multi-Messenger Observations of Gravitational Wave Sources" (Grant Number 24103005). This work was also supported in part by MEXT Grant-in-Aid for Scientific Research (C) (Grant Number 15K05071; K. Oohara), by JSPS Grant-in-Aid for Young Scientists (B) (Grant Number 26800129; H.Takahashi).

References

1. N. E. Huang *et al.*, *Proc. R. Soc. London, Ser. A* vol.**454**, pp.903–993 (1998).
2. H. Takahashi, K. Oohara, M. Kaneyama, Y. Hiranuma, and J. B. Camp, Advances in Adaptive Data Analysis **5**, 2 (2013).
3. H. Dimmelmeier *et al.*, *Phys. Rev. D* **78**, 064056 (2008)
4. https://dcc.ligo.org/cgi-bin/DocDB/ShowDocument?docid=2974.
5. Z. Wu and N. E. Huang, *Advances in Adaptive Data Analysis* **1**, pp.1–41 (2009).